Journal of the Korean Physical Society, Vol. 42, February 2003, pp. S642∼S646

Analytic Model for Photo-Response of p-Channel MODFET'S

Hwe-Jong KIM,* Ilki HAN, Won-Jun CHOI, Young-Ju PARK, Woon-Jo CHO and Jung-Il LEE†
Nano Device Research Center, Korea Institute of Science and Technology, Seoul 130-650

Dong-Myong KIM
School of Electrical Engineering, Kookmin University, Seoul 130-302

Jacques ZIMMERMANN
IMEP, CNRS/INPG, 23 rue des martyrs, 38016, Grenoble, France

In this article we propose a comprehensive physical model for the photo-response of MODFET's and analyze the experimental results for p-channel InGaP/GaAs/InGaAs double heterojunction pseudomorphic MODFET's. The analytic model is based on the quantum nature of the two-dimensional carrier statistics in the channel and the recently developed device equation for the gate current. The model predicts a power law relationship between the current ratio with and without optical illumination, and the optical intensity, and successfully explains the experimental results. The gate voltage dependence of the effective ideality factor for the whole gate structure was extracted and discussed.

PACS numbers: 73.40.-c
Keywords: MODFET's, Photo-response, Gate current, Ideality factor, Threshold Voltage, Drain current, Two-dimensional electron (hole) gas

I. INTRODUCTION

Research on the photo-responses of microwave devices has attracted a lot of interest due to their possible application for future high-speed fiber-over-radio communication systems. Photo-responses of microwave devices such as metal-semiconductor field effect transistors (MESFET's), high electron mobility transistors (HEMT's), modulation doped field effect transistors (MODFET's), and heterojunction bipolar transistors (HBT's) were intensively studied both theoretically and experimentally [1–14]. In MODFET's, however, most of the work concentrated on n-channel devices [1–7]. The nonlinear behavior of the threshold voltage upon optical illumination was explained by the two-dimensional quantum nature of the electrons in the channel [1]. Effect of optical illumination on the Schroedinger wave function of the carriers has been calculated and the analysis was extended to the modified optical signal [2–4]. Parallel conduction in the barrier layer and modulation of the effective channel length in the saturation region due to the optical stimulation has been discussed and the photo-responses of MESFET's and MODFET's were compared [5–7]. p-channel devices suffer from low hole mobility, resulting in smaller photo-response compared to n-channel devices. However, the study of p-channel devices is important when complementary circuits are necessary, then, the performance of the circuit would be limited by the performance of the p-channel devices. Kim et al. reported for the first time the optical response of the p-channel InGaP/GaAs/InGaAs double heterojunction pseudomorphic MODFET's for both DC and microwave characteristics [8–10]. Analysis of these optical responses continued [11–14] and Kim, in particular, found a semi-empirical relation (a power law) between the responsivity for both the gate current and drain current, and the optical power intensity [12], not only in p-channel MODFET's but also in n-channel MODFET's and MESFET's. In this report, we present a simple physical model to explain the photo-response behavior of the gate current and the drain current of the p-channel MODFET's, based on the quantum nature of the two-dimensional hole gas in the channel and a new analytic model for the gate current. The new gate current model is based on previous work by others [15–19] and gives in an explicit expression for the current-voltage relation and the variation of the effective ideality factor of the whole gate structure [20]. The photo-response of the device becomes maximal near the threshold region in saturation where the conduction mechanism changes from drift to diffusion. The experimental results are compared to the analytical models based on physical understanding of the photo-detection mechanisms. The developed model can be applied to both n-channel and p-channel MODFET's and the basics of the model are

*Now at KOPTL
†E-mail: jil@kist.re.kr

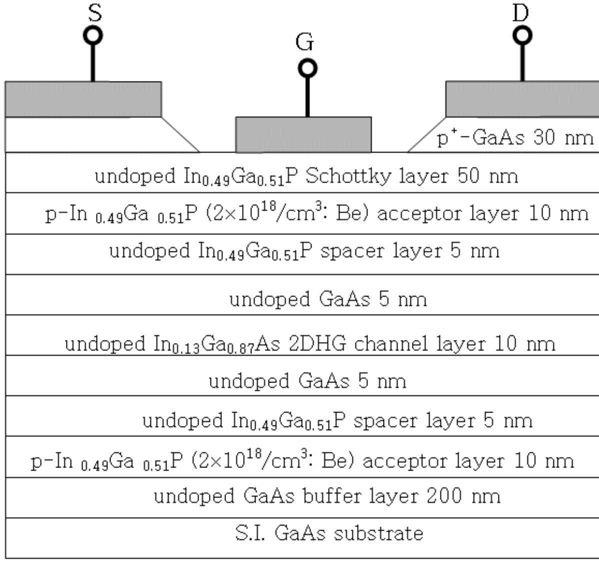

Fig. 1. Device structure for an p-channel MODFET.

stated for n-channel device for convenience.

II. DEVICE

The epitaxy layers of the device structure are schematically depicted in Fig. 1. The layers were grown on semi-insulating GaAs substrate by gas source molecular beam epitaxy. The growth sequence is as follows; 200 nm undoped GaAs buffer layer, 10nm p-type $In_{0.49}Ga_{0.51}As$ acceptor layer (2×10^{18} / cm^3 : Be), 5 nm undoped $In_{0.49}Ga_{0.51}$ spacer layer, 5 nm undoped GaAs spacer layer, 10 nm undoped $In_{0.13}Ga_{0.87}As$ channel layer, 5 nm undoped GaAs spacer layer, 5nm undoped $In_{0.49}Ga_{0.51}P$ spacer layer, 10 nm p-type $In_{0.49}Ga_{0.51}As$ acceptor layer(2×10^{18} /cm^3 :Be), 50 nm undoped $In_{0.49}Ga_{0.51}P$ Schottky barrier layer, 30 nm p^+-GaAs(3×10^{19} /cm^3 :Be) cap layer for ohmic contact. The structure is symmetric double heterojunction. The gate area was wt etched down to the Schottky barrier layer, and the Schottky gate contact (Ti/Au) and ohmic contact (Au-Zn/Cr/Au) were fabricated. The gate length of 1 μm, gate width of 240 μm (p-shaped), and gate-drain/source spacing of 1.5 mm were defined and PECVD-SiN_x passivation finished for the device structure fabrication. The channel carrier density and the mobility of the holes were measured to be 1.9×10^{12} /cm^2 and 250 cm^2 /V at room temperature, and 1.9×10^{12} /cm^2 and 5800 cm^2 /V at 23 K, respectively, confirming the two-dimensionality of the channel carriers. Current-voltage characterization was done utilizing a HP4156A semiconductor parameter analyzer with 800 nm laser diode as the light source. The optical power of the laser diode was varied up to 20 mW, which gave in 2.15 mW at the end of the fiber.

III. CARRIER STATISTICS

The carrier density in the channel is given by the sum of carriers in the quantized energy levels weighted by the wave function [21–23]. Assuming only the first subband is occupied, the carrier statistics governing the carrier density n_s, in the two-dimensional channel and the Fermi level E_F, can be approximated as follows,

$$n_s = DkT\Big(1 + e^{\frac{E_F - E_0}{kT}}\Big), \tag{1}$$

where $D = 4\pi m^*/h^2$, is the two-dimensional density of states and E_0 is the ground state energy. Photogenerated carriers alternate the Fermi level according to this relation, sometimes called the internal photovoltaic effect. For E_F -$E_0 \ll$ kT, one gets the change in the Fermi level after illumination such that [1],

$$E'_F - E_F = kTln\Big(1 + \frac{P}{P_0}\Big), \tag{2}$$

where E'_F is the Fermi level with optical illumination of optical power intensity P, and P_0 is the parameter indicating the onset of the saturation which can be obtained from the charge neutrality and the increment of the carrier density. P_0 is related to the material and the geometry of the device and inversely proportional to the minority carrier lifetime. Considering the gate capacitance which relates the band bending in the channel layer to the total charge, one can easily show that the induced photovoltage, V_{ph}, is equivalent to the Fermi level shift, in strong inversion where the depletion term in the capacitance can be neglected, such that,

$$qV_{ph} = \Delta E_F \equiv E'_F - E_F. \tag{3}$$

The photovoltage manifests itself as the threshold voltage shift. The measured threshold voltage shift from the square root of drain current vs. optical power intensity is shown in Fig. 2. The nonlinear optical intensity dependence of the threshold voltage has been experimentally observed by many authors [1]. The photovoltage can be also viewed as the additional gate voltage due to the optical illumination. From the shift of the threshold voltage in Fig. 2, the value of P_0 was determined to be about 13 mW.

IV. GATE CURRENT

In n-channel devices, for positive gate bias, diode 1 (gate/barrier) is under a forward biasing condition and diode 2 (barrier/channel) is under a reverse biasing condition. Neglecting series resistances and parallel conduction, the current transport in a Schottky diode can be

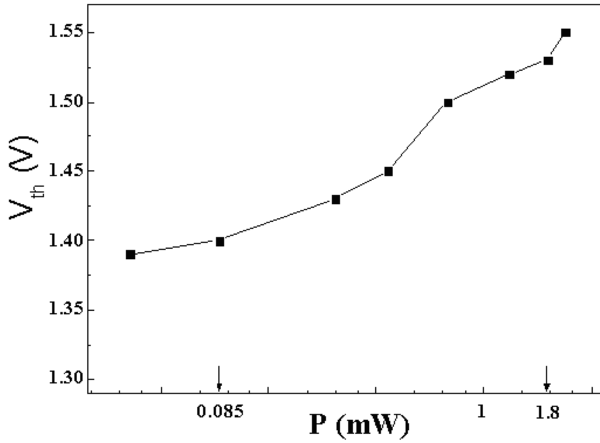

Fig. 2. Variation of threshold voltage, V_{th} (ΔV_{th}=V_{ph}), with optical power intensity, P.

described by thermionic emission theory at room temperature as follows [20],

$$I_g = I_{01}\Big(e^{\frac{qV_1}{n_1 kT}} - 1\Big), \tag{4}$$

$$I_g = -I_{02}\Big(e^{-\frac{qV_2}{n_2 kT}} - 1\Big), \tag{5}$$

$$V_g = V_1 + V_2, \tag{6}$$

The relation between the gate current I_g, and the gate bias V_g, can be easily derived as,

$$I_g = I_{01}\Big(e^{\frac{qV_g}{nkT}} - 1\Big). \tag{7}$$

The ideality factor, n, of the whole structure is determined by the ideality factors n_1 and n_2, of diodes 1 and 2, and the saturation current I_{01} and I_{02}, of diodes 1 and 2, respectively, such that,

$$n = n_1\left[1 + \frac{n_2}{n_1}\frac{ln\Big(\frac{I_{02}}{I_{02}-I_g}\Big)}{ln\Big(\frac{I_g+I_{01}}{I_{01}}\Big)}\right], \tag{8}$$

The saturation currents for the diodes exponentially depend on the negative of the barrier heights, sometimes called the diffusion potentials, ϕ_1 and ϕ_2, respectively, such that,

$$I_{0i} = WLA^{**}e^{\frac{-q\phi_i}{kT}}, i = 1, 2, \tag{9}$$

where WL(width times length of the gate) is the area of the diode (gate area) and A^{**} is the effective Richardson constant [16]. The barrier height ϕ_1, at the diode 1 is known to be the difference between the metal work function and the electron affinity of the barrier semiconductor [24]. However, it is found that the Schottky barrier height has a strong correlation with the heterojunction band offset in a metal/III-V compound semiconductor system [25]. The barrier height ϕ_2 is simply the difference between the conduction band edge of the barrier semiconductor at the heterointerface E_C and the Fermi level at the channel E_F, such that,

$$q\phi_2 = E_C - E_F. \tag{10}$$

The barrier height ϕ_2, decreases as the gate bias increases. Since ϕ_1 is usually much larger than ϕ_2, the saturation current of the diode 1 is several orders of magnitude smaller than that of the diode 2. From eqn. 6, one can see that the ideality factor of the gate current can be approximated as n_1 for $I_g << I_{02}$. However, if the barrier heights have comparable values, the ideality factor will increase. In general, ΔE_c and then $q\phi_2$ is known to be smaller than $q\phi_1$. If they have the same barrier heights, such as in strong inversion, then eq. 6 gives the ideality factor equal to $n_1 + n_2$.

As the drain bias is increased, the potential along the gate length of the channel cannot be treated as the same, and the bias condition for the gate structure becomes position-dependent. One has to consider the distributive nature of the gate current as has been discussed by Ruden *et al.* [18], which is also responsible for the negative transconductance at high gate voltages. The gate-channel current arises from a distributed current density with the position-dependent channel potential $V(x)=V_d(x/L)$, such that,

$$\delta I_g = I_{01}\Big[e^{\frac{q(V_g - V(x))}{nkT}} - 1\Big](\frac{\delta x}{L}), \tag{11}$$

where x is the coordinate along the channel from the source. Now the gate current in saturation region can be obtained by integration of eqn. 8 throughout the gate length. The result gives,

$$I_g = I_{01}\Big[\Big(\frac{nkT}{qV_d}\Big)e^{\frac{qV_g}{nkT}} - 1\Big], \tag{12}$$

for $qV_d>>nkT$. Note that the gate current decreases with the increase of the drain voltage. In doing the integration we neglected the gate voltage dependence of the ideality factor, which can be justified by the fact that the gate current near the source contributes most and the gate current near the drain side does not contribute to the total gate current due to the different channel potential. The ideality factor for the given gate bias in the linear region as given by eqn. 5 can safely represent the total ideality factor. For the gate current change due to the optical illumination in the saturation region, we utilize eqn. 9 where the photovoltage is added to the gate voltage, such that,

$$I'_g = I_g(V_g + V_{ph}) = I_{01}\left(\frac{I_g + I_{01}}{I_01}e^{\frac{qV_{ph}}{nkT}} - 1\right). \tag{13}$$

In strong inversion, the gate current is much larger than the saturation current for the diode 1 ($I_g>>I_{01}$),

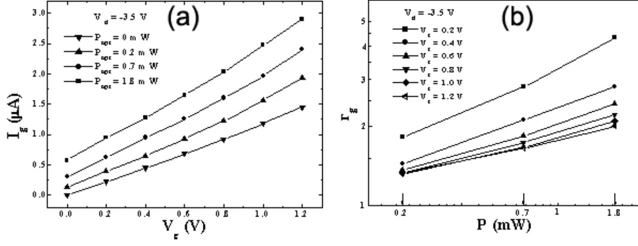

Fig. 3. (a) Gate current vs. gate voltage in the saturation region foe different optical illumination intensities (b) The optical power intensity dependence of the ratio of gate currents with and without optical illumination at different gate voltages in the saturation region.

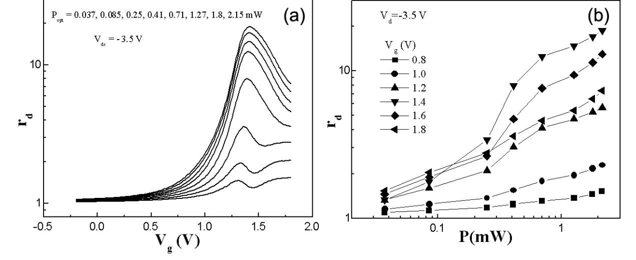

Fig. 4. (a) Gate voltage dependence of the drain current ratio, rd, for different optical intensities (b) Optical power intensity dependence of the ratio of the drain currents with and without optical illumination, for different gate voltages near the threshold.

and one can obtain the ratio r_g, of the gate currents with and without optical illumination as follows,

$$r_g \equiv \frac{I'_g}{I_g} = \Big(1 + \frac{P}{P_0}\Big)^{\frac{1}{n}}, \tag{14}$$

When $P >> P_0$, plotting $\ln r_g$ vs. $\ln(P/P_0)$, one can determine the ideality factor for the given gate voltage from the slope. Fig. 3(a) shows the gate voltage dependence of the gate current in the saturation region (V_d = -3.5V) for three different optical intensities (P = 0, 0.2, 0.7, 1.8 mW). The optical intensity dependence of the gate current for different gate voltages is shown in Fig. 3(b). The log-log plot in Fig. 3(b) enables the determination of ideality factor for a given gate voltage. One can see that the ideality factor increases as the gate voltage increases from 0.2 V to 1.2 V. The values for n were 2.76, 3.51, 4.06, 4.64, 5.0, 5.42 for V_g = 0.2, 0.4, 0.6, 0.8, 1.0, 1.2 V, respectively. This increase in the effective ideality factor, n, can be understood using eq. 5 where at low gate voltage, most of the gate bias is applied to the diode 1 and the effective ideality factor can be represented by n_1 and as the gate bias increases, n becomes the combination of n_1 and n_2 , and becomes larger.

V. DRAIN CURRENT (SUBTHRESHOLD)

The subthreshold current of a MODFET can be described as follows,

$$I_{ds} = K_3\Big(1 - e^{\frac{qV_d}{kT}}\Big)e^{\frac{q(V_g - V_{th})}{mkT}}, \tag{15}$$

where we approximated the surface potential as the gate bias, (V_g - V_{th}) in the last term with an experimental constant m similar to the ideality factor. When the drain bias is large enough, the drain voltage term can be neglected. The ratio r_d , of the drain current with and without optical illumination can be expressed in the same way as eq. (14)

$$r_d \equiv \frac{I'_{ds}}{I_{ds}} = \Big(1 + \frac{P}{P_0}\Big)^{\frac{1}{m}}. \tag{16}$$

The gate voltage dependence of the ratio for different optical intensities is presented in Fig. 4(a). The ratio reaches a maximum near threshold voltage and decreases as the gate voltage increases deeper into the subthreshold region. The parameter m for the other gate voltages can be considered as comparable to the ideality factor extracted from the optical power intensity dependence of the gate current. However, as the gate bias increases, the ideality factor should increase as predicted by eq. (5) and experimentally shown in Fig. 3(b). The decrease of the value of m at voltages larger than 1.25 V (Fig. 4(b)) seems to be due to the enlarged photovoltage near the threshold and subthreshold region. Note that the photovoltage was extracted in the strong inversion region

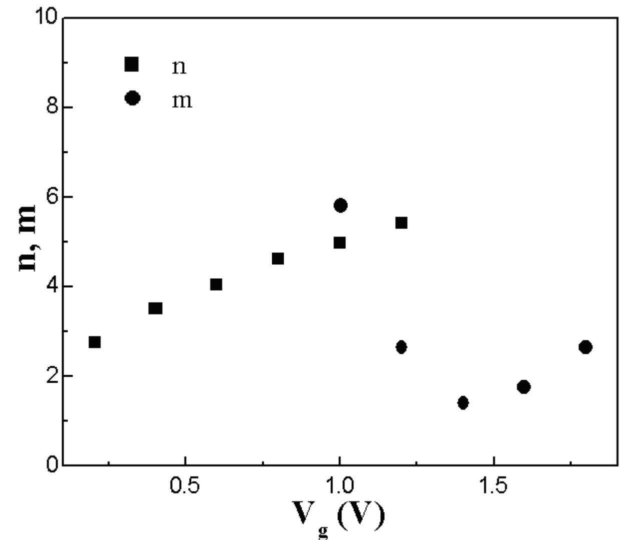

Fig. 5. Ideality factor for the gate structure vs gate voltage, obtained from photo-response of gate currents, Fig. 3 (n, solid squares), and from saturated drain current, Fig. 4 (m, solid dots).

and may not be appropriate to be used in the threshold region. It seems that the extra photovoltage induced at the depleted region compensated the large ideality factor and the reduced value for m is observed. In Fig. 5, the ideality factors obtained from the gate current variation (solid squares) and drain current variation (solid dots) are plotted as a function of the gate voltage.

VI. SUMMARY

We have developed a simple physical model explaining the change in the gate current and drain current with optical illumination intensity. The model considers the gate current path as two Schottky diodes in series back-to-back. Utilizing the quantum carrier statistics for the two-dimensional carriers in the channel, it is shown that the photogenerated carriers modifiy the Fermi level and equivalently the diffusion potential of the second diode which increases the gate current. From the model, we find a simple power law relationship between the gate and drain current ratios with and without optical illumination, and the illuminated optical intensity. Experimental results were analyzed with the model successfully providing more insights to the photodetection mechanism of p-channel MODFET's. The power index was related to the ideality factor of the gate structure. The drain current near threshold in the saturation region was found to be most sensitive to the optical stimulation with the ratio of the drain currents with and without illumination reaching almost 20. The model can be applied to the analysis on n-channel [26–32] in a similar manner. This work can be useful in implementing a circuit simulator for MODFET's as photodetectors.

ACKNOWLEDGMENTS

This work was partially supported by the Ministry of Science and Technology through NRL program (IKH) and the Ministry of Information and Communication through Advanced Backbone Technology Development Program.

REFERENCES

[1] M. A. Romero, M. A. G. Martinez and P. R. Herczfeld, IEEE Trans. Microwave Theory and Tech. **44**, 2279 (1996).
[2] H. Mitra, B. B. Pal, S. Singh and R. U. Khan, IEEE Trans. Electron Dev. **45**, 68 (1998).
[3] P. K. Singh and B. B. Pal, J. Appl. Phys. **88**, 4325 (2000).
[4] P. K. Singh and B. B. Pal, Solid-St. Electron. **43**, 1833 (1999).
[5] D. M. Kim, G. M. Lim and H. J. Kim, Solid-St. Electron **43**, 934 (1999).
[6] D. M. Kim, S. H. Song, H. J. Kim and K. N. Kang, IEEE Electron Dev. Lett. **20**, 73 (1999).
[7] D. M. Kim, H. J. Kim, J. I. Lee and Y. J. Lee, IEEE Electron Dev. Lett. **21**, 264 (2000).
[8] H. J. Kim, S. H. Kim, J. I. Lee, K. N. Kang, D. M. Kim and K. Cho, Electron. Lett. **34**, 126 (1998).
[9] H. J. Kim, D. M. Kim, S. H. Kim, J. I. Lee, K. N. Kang and K. Cho, Jpn. J. of Appl. Phys. **37**, L322 (1998).
[10] H. J. Kim, D. M. Kim, D. H. Woo, S. I. Kim, S. H. Kim, J. I. Lee, K. N. Kang and K. Cho, Appl. Phys. Lett. **72**, 584 (1998).
[11] H. J. Kim, D. M. Kim, J. I. Lee and J. Zimmermann, *SPIE Proc.* (San Jose, Jan., 2000), p. 3944.
[12] D. M. Kim, Appl. Phys. Lett. **77**, 4043 (2000).
[13] I. K. Han, H. J. Kim, D. M. Kim and J. I. Lee, 2nd JKJ-MWP, (Yonsei Univ., Seoul, Feb., 2001).
[14] H. J. Kim, D. M. Kim, I. K. Han, W. J. Choi, J. Zimmermann and J. I. Lee, *AWAD2002*, (Hokkaido Univ., Sapporo, July, 2002), p. 241.
[15] P. P. Ruden, M. Shur, A. I. Akinwande and P. Jenkins, IEEE Trans. Electron Dev. **36**, 453 (1989).
[16] K. Y. Lee, B. Lund, T. Ytterdal, P. Robertson, E. J. Martinez, J. Robertson and M. S. Shur, IEEE Trans. Electron Dev. **43**, 845 (1996).
[17] Y. H. Byun, K. Lee and M. Shur, IEEE Electron Dev. Lett. **11**, 50 (1990).
[18] C.-H. Chen, S.M. Baier, D. K. Arch and M. S. Shur, IEEE Trans. Electron Dev. **35**, 570 (1988).
[19] T. Ytterdal, T. A, Fjeldry, M. S. Shur, S. M. Baier and R. Lucero, IEEE Trans. Electron Dev. **46**, 1577 (1999).
[20] I. K. Han, J. I. Lee, J. Brini and A. Chovet, J. Korean Phys. Soc. **39**, S322 (2001).
[21] D. Delagebaudeuf and N. T. Lihn, IEEE Trans. Electron Dev. **ED-29**, 955 (1982).
[22] T. J. Drummond, H. Morkoc, K. Lee and M. S. Shur, IEEE Electron Dev. Lett. **EDL-3**, 338 (1982).
[23] F. Stern and S. Das Sharma, Phys. Rev. B **30**, 840 (1984).
[24] S. M. Sze, *Physics of Semiconductor Devices* (New York, Wiley, 1981), Chap. 5, p. 247.
[25] J.-K. Lee, Y.-H. Cho, B.-D. Choe, K. S. Kim, H. I. Jeon, H. Lim and M. Razeghi, Appl. Phys. Lett. **71**, 912 (1997).
[26] J. Bunm and S.-W. Lee, J. Korean Phys. Soc. **37**, 313 (2000).
[27] J. H. kim and J.-I. Song, J. Korean Phys. Soc. **38**, 142 (2001).
[28] H. S. Yoon, J. H. Lee and K. H. Lee, J. Korean Phys. Soc. **39**, S275 (2001).
[29] S. D. Cho, H. T. Kim, S. J. Song, H. C. Kim, Y. C. Kim, S. K. Kim, D. J. Kim and D. M. Kim, J. Korean Phys. Soc. **40**, 577 (2002).
[30] J. Y. Shim, H. S. Yoon, S. J. Kim, J. Y. Hong, W. J. Chang, D. M. kang, J. H. Lee and K. H. Lee, J. Korean Phys. Soc. **41**, 528 (2002).
[31] S. W. Kim, H.-J. Park, S.-Y. Oh, D.-y. Ko, D.-H. Kim and K.-S. Seo, J. Korean Phys. Soc. **41**, 918 (2002).
[32] D. H. Kim, S.-Y. Oh, J.-J. Kim, J.-H. Lee, K.-W. Chung and K.-S. Seo, J. Korean Phys. Soc. **41**, 1036 (2002).